Journal of Applied Polymer Science

Synthesis of Polypropylene-Grafted Graphene and Its Compatibilization Effect on Polypropylene/Polystyrene Blends

Feng You,[1] Dongrui Wang,[1] Xinxin Li,[1] Meijing Liu,[1] Zhi-Min Dang,[1] Guo-Hua Hu[2]

[1]Department of Polymer Science and Engineering, School of Chemistry and Biological Engineering, University of Science and Technology Beijing, Beijing 100083, China

[2]CNRS-Université de Lorraine, Laboratoire Réactions et Génie des Procédés, UPR3349, ENSIC, 1 rue Grandville, BP 20451, Nancy, F-54000, France

Correspondence to: Z.M. Dang (E-mail: dangzm@ustb.edu.cn) and G.H. Hu (E-mail: guo-hua.hu@univ-lorraine.fr)

ABSTRACT: Polypropylene-*graft*-reduced graphene oxide (PP-*g*-rGO) was synthesized and used as a novel compatibilizer for PP/polystyrene (PP/PS) immiscible polymer blends. SEM observation revealed an obvious reduction of the average diameter for the dispersed PS phase with the addition of PP-*g*-rGO into a PP/PS (70/30, w/w) blend. The compatibilization effect of PP-*g*-rGO will subsequently lead to the enhancement of the tensile strength and elongation at break of the PP/PS blends. The compatibilizing mechanism should be ascribed to the fact that PP-*g*-rGO can not only adsorb PS chains on their basal planes through π-π stacking but also exhibit intermolecular interactions with PP through the grafted PP chains. © 2014 Wiley Periodicals, Inc. J. Appl. Polym. Sci. **2014**, *131*, 40455.

KEYWORDS: compatibilization; nanotubes; graphene and fullerenes; phase behavior

Received 5 November 2013; accepted 16 January 2014
DOI: 10.1002/app.40455

INTRODUCTION

Graphene, a well-known two-dimensional material, has drawn intensive attention since its first finding by Novoselov et al. in 2004.[1] Because of its superior electrical, thermal, and mechanical properties, graphene has become a very promising material for various applications.[2] To date, extensive studies have been reported on the preparation of graphene and its composites.[3–5] Graphene-filled polymer nanocomposites are very attractive for the simple reason that physical properties of polymers can be remarkably enhanced by incorporating only a small amount of graphene.[6,7] Over the past few years, many researchers have focused on developing effective strategies to fabricate high performance polymer/graphene nanocomposites.

Mixing two or three polymers is an efficient way to producing new multiphase materials with excellent ultimate properties. In fact, polymer blends have attracted intensive scientific and industrial interest during the past decades.[8,9] Unfortunately, most of polymers are immiscible with each other because of the positive Gibbs energy of mixing, which results in phase separation, poor adhesion in interfaces, and deteriorated ultimate properties. Therefore, compatibilization of the immiscible polymer pairs must be taken into full consideration during the design of a high-performance polymer blends. The simplest and most effective way to compatibilize immiscible polymers is using compatibilizers. Graft or block copolymers, prepared separately or produced *in situ* during blending, have been widely used as compatibilizers, for instance, polypropylene-*graft*-maleic anhydride (MAPP) compatibilizing polypropylene/polyamide (PP/PA) blends, polystyrene-*graft*-maleic anhydride (SMA) for polystyrene/polyamide (PS/PA) blends.

PP and PS are commodity polymers and form a typical example of immiscible polymer blends. The compatibilization is essential to balance their ultimate performances. Styrene-butadiene rubber, styrene-butadiene-styrene triblock copolymer (SBS), and styrene-ethylene/butylenes-styrene triblock copolymer (SEBS) have been used as compatibilizers for PP/PS blends for many years.[10–13] Recently, some functional inorganic nanofillers, including silica nanoparticles[14,15] and sodium montmorillonite (OMMT),[16,17] have also been developed for compatibilizing PP/PS blends. The high modulus and low cost make inorganic nanofillers very attractive in compatibilizing. Very recently, graphene oxide (GO) and its derivatives have been employed to compatibilize polymer blends by Cao et al.[18,19] In their pioneer work, amphiphilic GO can strongly interact with immiscible polymer pairs such as PA/polyphenylene oxide (PPO) and PP/PPO and enhance their interfacial adhesion, which results in improved compatibility and better mechanical strength. The π-π

Additional Supporting Information may be found in the online version of this article.

stacking effect between graphene (functionalized graphene) and aromatic rings of some polymers[19,20] can be used to improve the interfacial interaction. A remarkable reduction of interfacial adhesion in these immiscible polymer blends can be achieved by incorporating little amount of graphene. Since PS is often used in preparing polymer blends, it is of scientific and industrial interest to develop a compatibilization strategy for PP/PS blends by using graphene or GO nanosheets as the compatibilizer.

In this work, PP grafted reduced graphene oxide nanosheets (PP-*g*-rGO) is prepared by covalently bonding MAPP onto the surfaces of amino functionalized rGO. The PP-*g*-rGO nanosheets can adsorb PS chains on their basal planes through π-π stacking while exhibiting intermolecular interactions with PP through the grafted PP chains. The compatibilizing effect of PP-*g*-rGO on the phase morphology and mechanical properties will be presented in detail in the following parts.

EXPERIMENTAL

Materials

PP (T30S, MFI = 3.0 g/10 min) was purchased from Maoming Petroleum Chemical, China. PS (PS PG-383M, MFI = 3.0 g/10 min) was obtained from Zhenjiang Chi Mei Chemical, China. Polypropylene-*graft*-maleic anhydride (MAPP, GPM200B) with a maleic anhydride grafting ratio of 1.0 wt % was supplied by Ningbo Nengzhiguang New Materials Technology, China. Graphite powder (Sinopharm Chemical Reagent) with a size of 300–400 mesh was sieved out prior to use. All other reagents and solvents were analytical grade products and used without further purification.

Preparation of Amine Modified Reduced Graphene Oxide (rGO-NH_2)

Graphite oxide was prepared using natural graphite powders following a modified Hummers method. The procedures for the synthesis and characterization can be found elsewhere.[21,22] Dried graphite oxide (2.0 g) was dispersed in *N,N*-dimethylformamide (DMF, 1 L) to form a GO dispersion through exfoliation under ultrasonication. Ethylenediamine (40 mL) was then added to the dispersion and the mixture was heated at 90°C for 8 h and under vigorous stirring. The resulting suspension was filtered over a nylon membrane with a pore size of 1.20 μm and washed with excessive methanol. Finally, the obtained rGO-NH_2 powder was dried at 60°C under vacuum for 48 h and the weight of rGO-NH_2 powder was about 1.2 g.

Preparation of Polypropylene Grafted Reduced Graphene Oxide (PP-g-rGO)

PP-*g*-rGO was prepared by grafting MAPP onto rGO-NH_2 surface via an amidation reaction. First, rGO-NH_2 (0.8 g) was dispersed in *N*-methyl-2-pyrrolidinone (NMP, 400 mL) with the aid of ultrasonication, then the dispersion was heated to 120°C. Meanwhile, A MAPP solution was prepared by dissolving MAPP pellet (0.8 g) in xylene (320 mL) at 120°C. Then the rGO-NH_2 suspension was slowly added to the MAPP solution dropwise under vigour stirring. After heating at 120°C for 5 h, the suspension was gradually cooled to room temperature and fine powders were precipitated from the mixture. The precipitates were filtered, washed with hot xylene to remove unreacted MAPP chains, and dried under vacuum at 80°C for 48 h and the obtained PP-*g*-rGO powder was about 1.1 g.

Fabrication of PP-g-rGO Compatibilized PP/PS Blends

The PP-*g*-rGO compatibilized PP/PS blends were fabricated through a two-step procedures: melt blending of PS with PP-*g*-rGO, and subsequent melt compounding of PP and PS with the PS/PP-*g*-rGO masterbatch. In the first step, the PP-*g*-rGO powder (0.5 g) was mixed with PS (3.5 g) by using a Haake miniLab micro compounder (Thermo Fisher Scientific, USA) at 180°C with a screw speed of 60 rpm for 8 min, yielding a PS/PP-*g*-rGO masterbatch. In the second stage, the obtained masterbatch, PP, and PS were blended in the Haake miniLab micro compounder in the melt at 180°C with a screw speed of 60 rpm for another 8 min. Three nanocomposites samples were obtained: PP/PS/PP-*g*-rGO (69.5/30/0.5, w/w/w), PP/PS/PP-*g*-rGO (68.5/30/1.5, w/w/w) and PP/PS/PP-*g*-rGO (67.0/30/3.0, w/w/w). They were denoted as PP/PS/0.5PG, PP/PS/1.5PG, and PP/PS/3.0PG, respectively. For comparison, a PP/PS (70/30, w/w) blend without PP-*g*-rGO, and PP/PS blends compatibilized by rGO-NH_2 and MAPP were also prepared through similar procedures. The denotation and formulas to the blends are listed in Table I.

Characterization

X-ray diffraction (XRD) patterns were recorded by using a D/MAX 2500 system (Rigaku, Japan) with a Cu Kα radiation source(40 KV, 150 mA). Fourier transform infrared spectroscopy (FTIR) measurements were carried out by using a Nicolet 5700 spectrometer (Thermo Fisher Scientific, USA). Thermal gravimetric analysis (TGA) was performed on a HCT-3 system (Beijing Henven Scientific, China) with a heating rate of 10°C/min under nitrogen atmosphere. Images of the atomic force microscopy (AFM) of PP-*g*-rGO were obtained on a Dimension™ 3100 system (Bruker Corporation, Germany) in the tapping mode. The fracture surfaces of the PP/PS blends compatibilized by rGO-NH_2, MAPP and PP-*g*-rGO were observed by using a S4700 field emission scanning electron microscope (SEM, HITACHI, Japan) with an accelerating voltage of 20 kV. The samples were etched by tetrahydrofuran (THF) for 8 h to remove the dispersed PS phase and sputter-coated with gold before observations. The dispersed PS phase size and size distribution were obtained by statistics based on

Table I. The Formations of PP/PS/PG, PP/PS/PR, and PP/PS/PM Nanocomposites

Samples	PP/PS, wt/wt	PP-*g*-rGO, wt	rGO-NH_2, wt	MAPP, wt
PP/PS/0.5PG	69.5/30	0.5	0	0
PP/PS/0.5PR		0	0.5	0
PP/PS/0.5PM		0	0	0.5
PP/PS/1.5PG	68.5/30	1.5	0	0
PP/PS/1.5PR		0	1.5	0
PP/PS/1.5PM		0	0	1.5
PP/PS/3.0PG	67.0/30	3.0	0	0

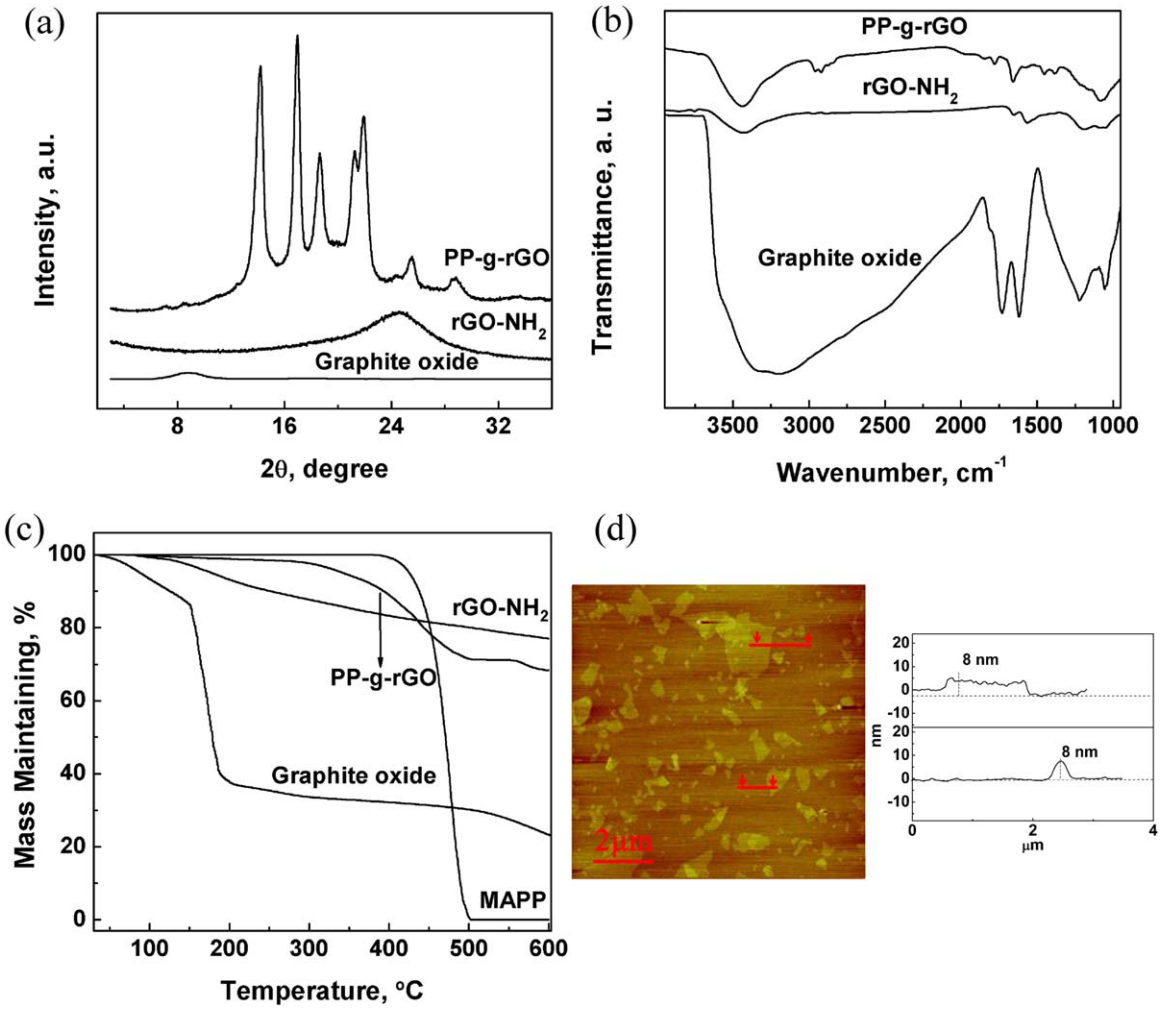

Figure 1. Structure characterizations of graphite oxide, rGO-NH_2 and PP-*g*-rGO: (a) X-ray diffraction patterns, (b) IR spectra, (c) TGA curves, and (d) AFM analysis of PP-*g*-rGO. [Color figure can be viewed in the online issue, which is available at wileyonlinelibrary.com.]

the SEM graphs. Typically, 300 particles were analyzed for each sample. The number-averaged diameter (D_a) was calculated by eq. (1).

$$Da = \frac{\sum_i N_i D_i}{\sum_i N_i} \quad (1)$$

where N_i is the number of particles with a diameter of D_i.

Mechanical properties of the PP/PS blends and PP/PS/PG nanocomposites were tested on an AG-IC Electronic Testing machine (SHIMADZU, Japan) at room temperature with a crosshead speed of 20 mm/min. The dumb-bell specimens with the dimension of 70 × 4 × 2 mm^3 were prepared by compression molding at 180°C under 15 MPa for 5 min. Six tests were performed for each sample and the values were averaged. The dynamic mechanical analysis (DMA) of samples was conducted on a DMA-Q800 (TA instruments, USA) machine with a tensile mode with a frequency of 1 Hz and a heating rate of 3°C/min within the range of −20°C to 120°C. The specimen dimensions of samples were 25 × 4 × 1 mm^3.

RESULTS AND DISCUSSION

Synthesis and Characterization of PP-g-rGO

It is well-known that graphene nanosheets or graphene oxide can exhibit strong interactions with PS chains through π-π stacking but poor interactions with nonpolar PP chains.[23] In this work, PP chains were grafted onto graphene surfaces and the resulting PP-*g*-rGO was used as a comatibilizer to improve the compatibility between PP and PS. As described in the experimental section, PP-*g*-rGO was prepared through an amidation reaction between amino groups on rGO-NH_2 and anhydrides on MAPP. The chemical structure and morphology of obtained PP-*g*-rGO were carefully characterized and the results are summarized in Figure 1.

It has been reported that graphite oxide consists of a layered structure of GO nanosheets with hydroxyl and epoxy groups on basal planes and carboxyl groups on edges.[24] Typical XRD pattern, IR spectrum, and TGA curve of the graphite oxide are displayed in Figure 1. XRD analysis shows that the interlayer distance of GO is about 0.99 nm ($2\theta = 8.9^\circ$). In its IR spectrum, peaks at 3350, 1735, 1620, and 1220 cm^{-1} correspond to the

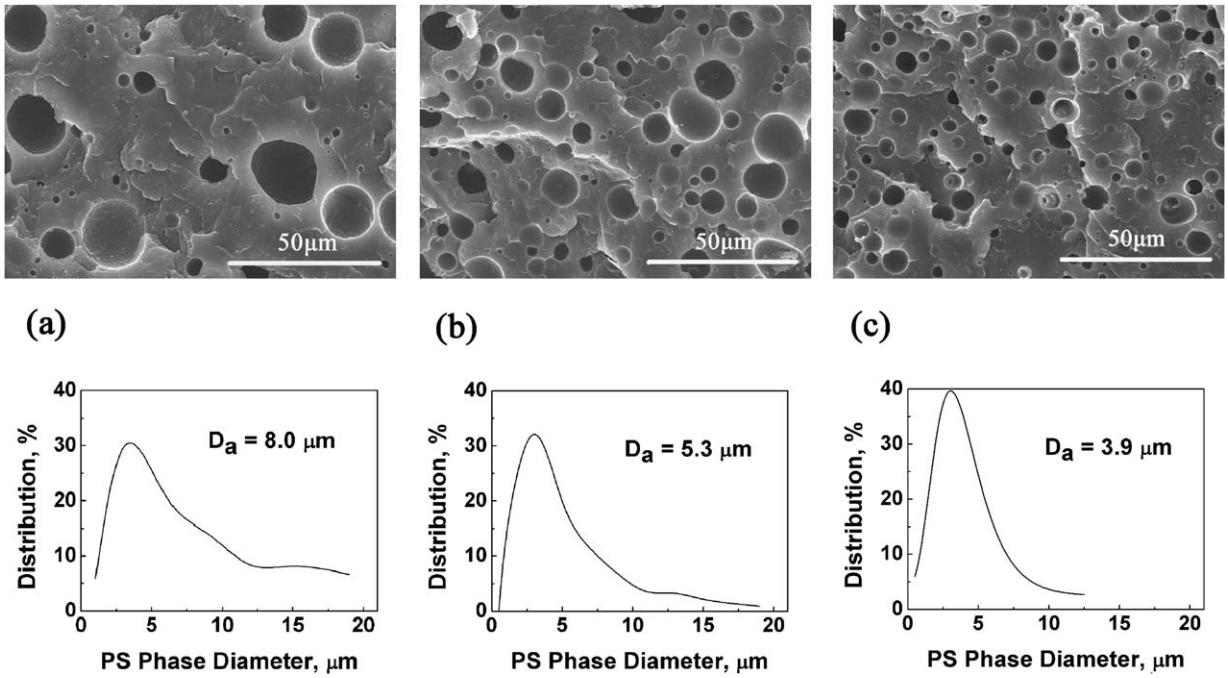

Figure 2. Typical SEM graphs of the fractured surfaces of PP/PS blends and PP/PS/PG nanocomposites, the dispersed PS phase was etched by THF for 8 h, below is the PS droplet diameter distribution: (a) PP/PS, (b) PP/PS/0.5PG, and (c) PP/PS/1.5PG.

O—H, C═O, C═C, C—O vibrations, demonstrating the existence of hydroxyl, epoxy, and carboxyl groups. After reaction with ethylenediamine, three new absorptions appear at 3435, 1653, and 1570 cm^{-1} while the peaks at 3350 and 1735 cm^{-1} vanish, indicating GO is partially reduced. The three new peaks correspond to the N—H stretching, N—H bending, and C═O stretching of rGO-NH_2. These observations clearly demonstrate that amino groups have been covalently bonded onto GO surfaces along with the reduction of GO induced by ethylenediamine.[25,26] Meanwhile, the XRD pattern of rGO-NH_2 shows a broad peak at $2\theta = 24.9^{\circ}$ and the corresponding interlayer distance is 0.34 nm, implying a restoration of graphitic structure in rGO-NH_2. This process can be further proved by TGA analysis. rGO-NH_2 shows a mass loss of 19.9% at 500°C, which is much lower than that of graphite oxide, revealing the removal of most oxygen-containing functional groups of rGO-NH_2 after reduced by ethylenediamine.

In the XRD pattern of PP-*g*-rGO, several new peaks at $2\theta = 14.0^{\circ}$, 16.8°, 18.5°, 21.1°, 21.8°, 25.6°, and 28.7° correspond to the crystalline planes of PP.[27] They have appeared after the grafting modification, revealing that MAPP chains have been

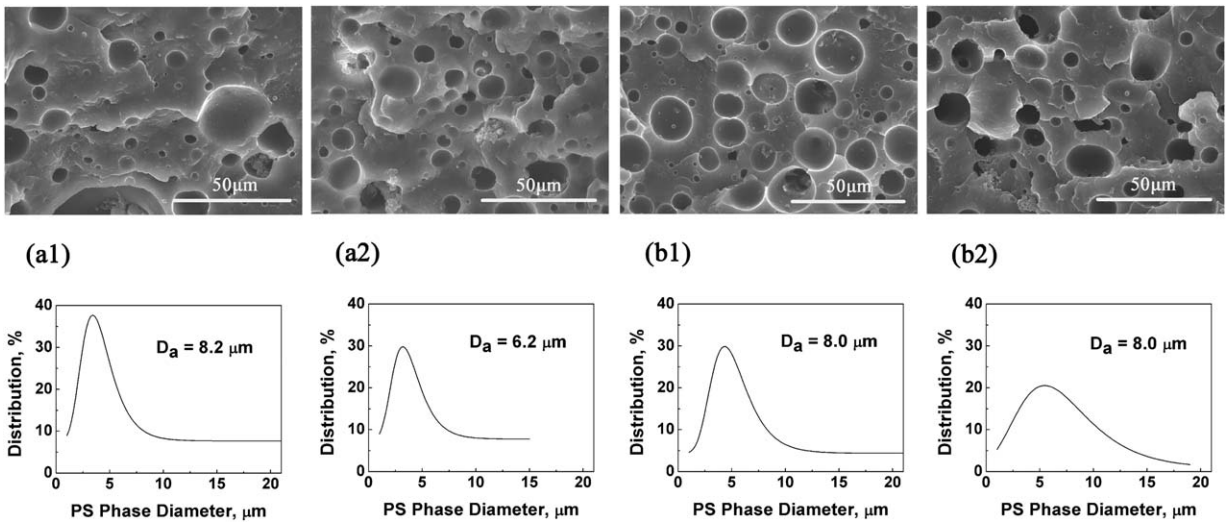

Figure 3. Typical SEM graphs of the fractured surfaces of PP/PS blends incorporated with rGO-NH_2 (PP/PS/PR) and MAPP (PP/PS/PM), the dispersed PS phase was etched by THF for 8 h, below is the corresponding PS droplet diameter distribution: a1 and a2 represent PP/PS/PR with 0.5 wt % and 1.5 wt % of rGO-NH_2; b1 and b2 represent PP/PS/PM with 0.5 wt % and 1.5 wt % of MAPP, respectively.

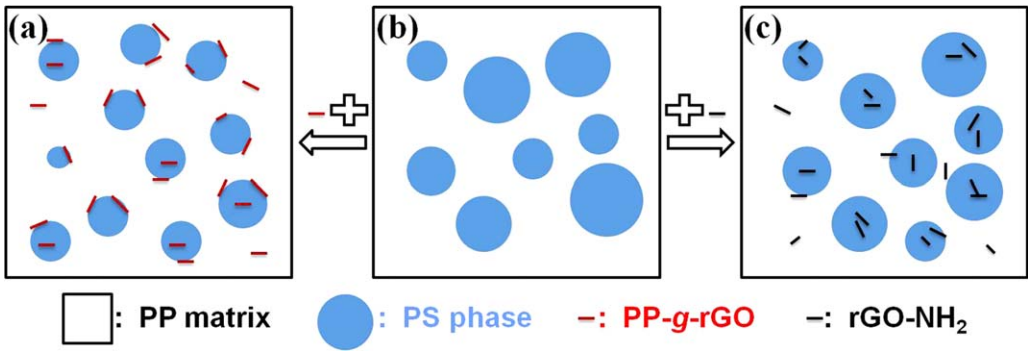

Figure 4. Schematic description of the compatibilizing effect of PP-*g*-rGO and rGO-NH_2 on PP/PS blends: (a), (b), and (c) represent PP/PS/PG nanocomposites, PP/PS blends, and PP/PS/PR nanocomposites, respectively. [Color figure can be viewed in the online issue, which is available at wileyonlinelibrary.com.]

successfully grafted onto rGO surfaces. In its IR spectrum, characteristic absorptions of PP such as the stretching vibration of —CH_2 at 2980 and 2920 cm^{-1} can be observed [Figure 1(b)]. Strong peaks at 1780 and 1464 cm^{-1} corresponding to the imide groups can also be observed, implying that the covalent grafting is successful through the reaction between the anhydride groups of MAPP and amino groups of rGO-NH_2.[28] The TGA curve of PP-*g*-rGO shows a mass loss of 28.5% at 500°C [Figure 1(c)]. Considering that MAPP can be totally decomposed at 500°C, the mass fraction of MAPP chains in PP-*g*-rGO should not exceed 28.5%. Figure 1(d) gives a typical AFM image of PP-*g*-rGO nanosheets. The average thickness of PP-*g*-rGO is ca. 8.0 nm, which is much higher than that of GO (0.8–1.2 nm).[29] Assuming that the MAPP chains are covalently bonded to both sides of rGO-NH_2, the height of PP-*g*-rGO is reasonable[30]. Similar results have also been reported by Cao et al.[19]

Compatibilization Effect of PP-g-rGO in PP/PS Blends

PP and PS are typical immiscible polymer blends among plastics, both of them have been widely used in many areas and played a significant role in polymer industry. Many methods have been developed to compatibilize PP/PS blends.[10,16] In this section, the compatibilization effect of obtained PP-*g*-rGO nanosheets on PP/PS blends was investigated. PP/PS (70/30, w/w) blends with different PP-*g*-rGO contents were first fabricated through melt blending. The changes in phase morphology of the samples as a function of PP-*g*-rGO content are depicted by Figure 2. The black domains indicate the position of the extracted PS phase. The SEM images of the PP/PS blends without PP-*g*-rGO show that the average diameter of dispersed PS phase is 8.0 μm. The addition of 0.5 wt % of PP-*g*-rGO nanosheets results in a remarkable decrease in the PS domain size to 5.3 μm. The average diameter of the PS domains can be further decreased to 3.9 μm upon the addition of 1.5 wt % of PP-*g*-rGO. Moreover, the diameter distribution of the PS domains tends to be more uniform along with the incorporation of PP-*g*-rGO, and the large PS agglomerates cannot be found in PP/PS blends when the content of PP-*g*-rGO reached 1.5 wt %. The SEM observations clearly demonstrate the positive compatibilization effect of PP-*g*-rGO nanosheets on PP/PS blends. The morphology behaviors of PP/PS blends compatibilized by rGO-NH_2 and MAPP (PP/PS/PR and PP/PS/PM) were also given in Figure 3 to further illustrate the compatibilization of PP-*g*-rGO in PP/PS blends. It can be seen that both rGO-NH_2 and MAPP have little effect on the dimension and distribution of dispersed PS phase. In addition, the effect of simultaneously incorporating rGO-NH_2 and MAPP on the morphology of PP/PS blends was also investigated. The results were shown as Figure S2 (Supporting information). Little differences have been found for the phase size of dispersed PS in PP/PS blends compatibilized with both rGO-NH_2 and MAPP. The possible reason to these phenomena caused by the different fillers can be described by using the schematic diagram shown as Figure 4. The PP-*g*-rGO nanosheets can absorb some PS chains on their graphene basal planes through π-π interactions.[20, 31] Meanwhile these nanosheets exhibit strong intermolecular interactions with PP phase due to the PP chains grafted on their surfaces. Thus the PP-*g*-rGO nanosheets tend to locate at the PP/PS interfacial regions, reducing unfavorable contacts and interfacial tensions. Consequently, the compatibility between PP and PS is improved and the size of the dispersed phase domains decreased. On the contrary, most of rGO-NH_2 can only locate in PS phase because of the π-π interaction [Figure 4(c)] and most of MAPP can locate in PP phase. Therefore, both rGO-NH_2 and MAPP have little effect on the reduction of interfacial tensions, leading to poor compatibilization for PP/PS blends.

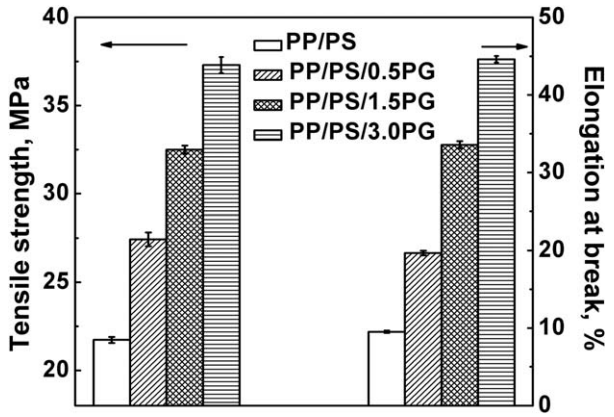

Figure 5. Tensile strength and elongation at break data of uncompatibilized PP/PS blends and PP-*g*-rGO compatibilized PP/PS blends.

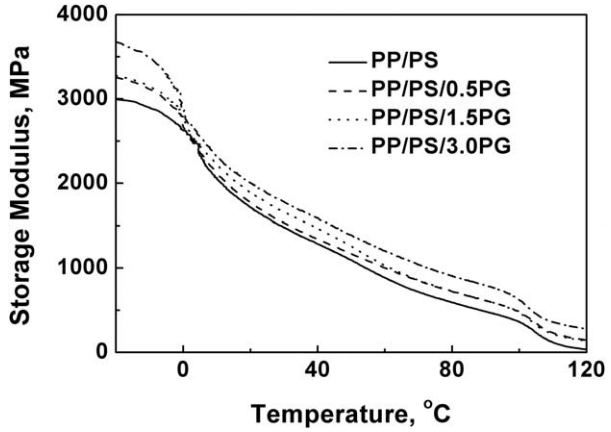

Figure 6. The storage modulus versus temperature curves for uncompatibilized PP/PS blends and PP-*g*-rGO compatibilized PP/PS blends.

However, by considering that both sides of the PP-*g*-rGO nanosheets were grafted with MAPP chains, the π-π stacking effect between them and PS chains should be partially alleviated due to the steric hinderance. Thus the compatibilization effect of graphene on PP/PS immiscible blends must have been partially deteriorated. A better compatibilization will be achieved if one can synthesize "Janus" graphene nanosheets with only one surface covalently functionalized by PP while another surface can exhibit strong interactions with PS through non-covalent π-π stacking.[32]

Generally, compatibilization can dramatically enhance the ultimate properties of immiscible polymer blends. The mechanical properties of PP/PS blends compatibilized by PP-*g*-rGO are given in Figure 5. The tensile strength and elongation at break of the PP/PS polymer blends are 21.7 MPa and 9.5%, respectively. The tensile strength of PP/PS blends without compatibilization is much lower than that of neat PP. (The tensile strength of PP is 35.3 MPa.) Moreover, the elongation at break of PP/PS blends is also very low. After the incorporation with PP-*g*-rGO, both the tensile strength and the elongation at break of the PP/PS blends are obviously enhanced. The tensile strength of PP/PS/1.5PG nanocomposites is nearly close to that of the neat PP. Both the tensile strength and elongation at break continue to increase when PP-*g*-rGO content is 3.0 wt%. Considering the fact that the content of PP-*g*-rGO nanosheets is lower than that of organic copolymer (the organic copolymer compatibilizer content in PP/PS blends is often higher than 5.0 wt%[10]), the improvement in mechanical properties of the PP/PS blends is remarkable. A possible reason to the improvement of mechanical properties is that the enhanced interfacial interaction among PP-*g*-rGO and the two polymers; the reduced PS particle size caused by the addition of PP-*g*-rGO also can promote interfacial stress transfer. It should be mentioned that PP-*g*-rGO can not only have compatibilizing effect on PP/PS blends but also increase their stiffness because of the high Young's modulus of graphene.[5] Figure 6 shows that the storage modulus of PP/PS/PG nanocomposites increase with the content of PP-*g*-rGO. Therefore, PP-*g*-rGO will be a promising multifunctional compitibilizer for PP/PS blends.

CONCLUSIONS

The compatibilization of immiscible PP/PS blends by using PP-*g*-rGO nanosheets was successfully realized in this work. The PP-*g*-rGO was prepared by grafting MAPP chains onto amino functionalized rGO nanosheets. SEM observation revealed an obvious reduction of the dispersed PS phase size in PP/PS (70/30 by weight) blends by incorporating only 1.5 wt% of PP-*g*-rGO. The tensile strength and the elongation at break of the PP/PS blends were also improved. Those results showed that PP-*g*-rGO can be a very promising compitibilizer to enhance ultimate properties of PP/PS blends. It is expected to be widely accepted and used in the near future.

ACKNOWLEDGMENTS

This work was financially supported by National Science Foundation of China (51103011), the Fundamental Research Funds for the Central Universities (FRF-TP-11-003B), and Beijing Municipal Natural Science Foundation (2132029).

REFERENCES

1. Novoselov, K. S.; Geim, A. K.; Morozov, S. V.; Jiang, D.; Zhang, Y.; Dubonos, S. V.; Grigorieva, I. V.; Firsov, A. A. *Science* **2004**, *306*, 666.
2. Cheng, S.; Chen, X.; Hsuan, Y. G.; Li, C. Y. *Macromolecules* **2012**, *459*, 993.
3. Lotya, M.; King, P. J.; Khan, U.; De, S.; Coleman, J. N. *ACS Nano* **2010**, *4*, 3155.
4. Wang, G. X.; Yang, J.; Park, J. S.; Gou, X. L.; Wang, B.; Liu, H.; Yao, J. *J. Phys. Chem. C.* **2008**, *112*, 8192.
5. Loh, K. P.; Bao, Q. L.; Ang, P. K.; Yang, J. X. *J. Mater. Chem.* **2010**, *20*, 2277.
6. Hsiao, M.C.; Liao, S. H.; Yen, M. Y.; Teng, C. C.; Lee, S. H.; Pu, N. W.; Wang, C. A.; Sung, Y.; Ger, M. D.; M. Ma, C. C.; Hsiao, M. H. *J. Mater. Chem.* **2010**, *20*, 8496.
7. Song, P. A.; Cao, Z. H.; Cai, Y. Z.; Zhao, L. P.; Fang, Z. P.; Fu, S. Y. *Polymer* **2011**, *52*, 4001.
8. Sengupta, P. M.; Noordermeerm J. W. *Polymer* **2005**, *46*, 12298.
9. Sengers, W. G. F.; Sengupta, P.; Noordermeer, J. W. M.; Picken, S. J.; Gotsis, A. D. *Polymer* **2004**, *45*, 8881.
10. Horák, Z.; Fořt, v.; Hlavatá, D.; Lednický, F. *Polymer* **1996**, *37*, 65.
11. Santana, O. O.; Müller, A. J. *Polym. Bull.* **1994**, *32*, 471.
12. MacauÇbas, P. H. P.; Demarquette, N. R. *Polymer* **2001**, *42*, 2543.
13. Halimatudahliana, Ismail, H.; Nasir, M. *Polym. Test.* **2002**, *21*, 163.
14. Zhang, Q.; Yang, H.; Fu, Q. *Polymer* **2004**, *45*, 1913.
15. Elias, L.; Fenouillot, F.; Majeste, J. C.; Cassagnau, P. *Polymer* **2007**, *48*, 6029.
16. Wang, Y.; Zhang, Q.; Fu, Q. *Macromol. Rapid. Commun.* **2003**, *24*, 231.
17. Sinha, R. S.; Pouliot, S.; Bousmina, M.; Utracki, L. A. *Polymer* **2004**, *45*, 8403.
18. Cao, Y. W.; Zhang, J.; Feng, J. C.; Wu, P. Y. *ACS Nano* **2011**, *5*, 5920.

19. Cao, Y. W.; Zhang, J.; Feng, J. C.; Wu P. Y. *J. Mater. Chem.* **2012**, *22*, 14997.
20. Yang, M. J.; Koutsos, V.; Zaiser, M. *J. Phys. Chem. B.* **2005**, *109*, 10009.
21. Hummers, W. S.; Offeman, R. E. *J. Am Chem. Soc.* **1958**, *80*, 1339.
22. Wang, D. R.; Bao, Y.R.; Zha, J. W.; Zhao, J.; Dang, Z. M.; Hu, G. H. *ACS Appl. Mater. Interface.* **2012**, *4*, 6273.
23. Wan, C. Y.; Chen, B. Q. *J. Mater. Chem.* **2012**, *22*, 3637.
24. Dreyer, D. R.; Park, S. J.; Bielawski, C. W.; Ruoff, R. S. *Chem. Soc. Rev.* **2010**, *39*, 228.
25. Shin, H. J.; Kim, K. K.; Benayad, A.; Yoon, S. M.; Park, H. K.; Jung, I. S.; Jin, M. H.; Jeong, H. K.; Kim, J. M.; Choi, J. Y.; Lee, Y. H. *Adv. Funct. Mater.* **2009**, *19*, 1987.
26. Che, J. F.; Shen, L. Y.; Xiao, Y. H. *J. Mater. Chem.* **2010**, *20*, 1722.
27. Xia, H. S.; Wang, Q.; Li, K. S.; Hu, G. H. *J. Appl. Polym. Sci.* **2004**, *93*, 378.
28. Scott, C.; Macosko, C. *J. Polym. Sci. Part B.* **1994**, *32*, 205.
29. Hassan, H. M. A.; Abdelsayed, V.; Khder, A. E. R. S.; AbouZeid, K. M.; Terner, J.; EI-Shall, M. S.; Al-Resayes, S. I.; El-Azhary, A. A. *J. Mater. Chem.* **2009**, *19*, 3832.
30. Fang, M.; Wang, K. G.; Lu, H. B.; Yang Y. L.; Nutt, S. *J. Mater. Chem.* **2010**, *20*, 1982.
31. Zhang, W. L.; Liu, Y. D.; Choi, H. J. *J. Mater. Chem.* **2011**, *21*, 6916.
32. Zhao, N.; Gao, M. Y. *Adv. Mater.* **2009**, *21*, 184.